

Active-Tuned Plasmonic Angle Modulator of Light Beams for Potential Application of 3D Display

Haibo Li,[†] Shuping Xu,[†] Hailong Wang,[†] Yuejiao Gu,[†] John R. Lombardi,[‡] and Weiqing Xu^{*†}

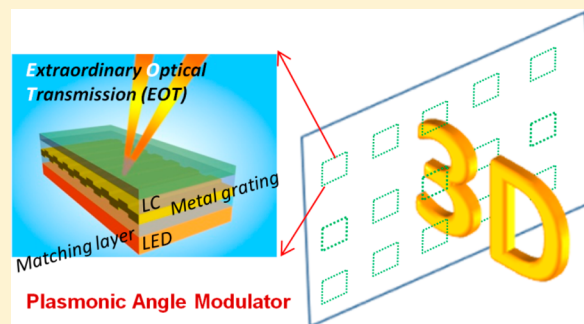
[†]State Key Laboratory of Supramolecular Structure and Materials, Jilin University, Changchun 130012, People's Republic of China

[‡]Department of Chemistry, City College of New York, New York, 10031, United States

S Supporting Information

ABSTRACT: We propose a plasmonic angle modulator device based on the extraordinary optical transmission (EOT) phenomenon combined with the liquid crystal (LC)-tuned surface plasmons (SPs). The configuration of this angle modulator mainly involves an Ag nanograting film for the SP coupling and a LC layer for continuously tuning SPs via voltage signals. Accordingly, the directions of the transmission light through the Ag nanograting film can be tuned continuously, realizing a light beam scanning in a 5° range at an operation rate of 60 Hz. We expect this active-tuned plasmonic angle modulator would have potential applications in three-dimensional (3D) display techniques that strictly require the elaborate and rapid angle modulation of light beams. In addition, this active-tuned plasmonic angle modulator can also be applied in other fields, such as photocommunication, optical detection, beam steering, and so on.

KEYWORDS: plasmonics, beam steering, liquid crystals, extraordinary optical transmission, 3D display, active modulation



Surface plasmons (SPs) can steer light in nanoscale due to their predominant capability of light control in subwavelength scale,^{1–5} which makes the angle modulation of light beams beyond the diffraction limit possible. In order to manipulate light beams, various plasmonic angle modulators have been developed, for example, nano-optical Yagi-Uda antennas and subwavelength apertures.^{2–5} The “static” modulation of light beams could be attained by tuning the geometric features of the plasmonics elements.^{6–8} However, the “active” control of the light is more attractive since it will be quite useful in further applications of photocommunication and optical detection. To achieve the active control in a plasmonic element, the basic nature that SPs are sensitive to the changes of the refractive indices (RIs) of the surrounding medium was commonly considered⁹ and the active modulation could be achieved by integrating SPs with electro-optical materials, for example, liquid crystals (LC).^{10–14} The active-tuning strategies exhibit superiorities in flexibility and maneuverability over the static SP tailoring methods, especially in the aspects of continuous, reversible, and swift modulation. Therefore, the active-modulated plasmonic elements are promising and may open up new opportunities to remedy the missing link between light and electrical signal in micronano scale. Recently, several active micro-optical elements based on this strategy have been proposed, such as nano photoswitches and wavelength-tunable light sources.^{15,16} However, the nanoscale electric-controlled beam angle modulator, which is important for the developments of photocommunication, optical detection, and so on, is still absent.

In this work, we propose an active angle modulator of light beams based on the LC-tuned SPs. We modulated the beam angles based on the plasmon-induced extraordinary optical transmission (EOT) phenomenon.^{17–19} The EOT effect on a thick metal film with periodic nanostructures (e.g., nano holes, nano slits, nanograting, etc.) is generally determined by the characteristics of SPs,^{20,21} leading to the selective transmission of rays at the SP resonance (SPR) angles. In this design, the SPR angles were tuned by the LC via voltage signals. Consequently, the directions of transmission beam were continuously modulated. The light beam scanning on this LC-tuned plasmonic device could be practical in displaying three-dimensional (3D) images.

RESULTS AND DISCUSSION

Principle and Design of the Angle Modulator of Light Beams. Figure 1a shows the schematic diagram of the angle modulator. Briefly, it contains a light emitting diode (LED) light source, a RI matching layer (RI = 1.70, about 100 nm in thickness), a 100 nm thick Ag film with a grating structure, and a LC layer (nematic LC, RI = 1.52–1.71). The both sides of the Ag nanograting has the same structure with a period of 320 nm and a depth of 25 nm from its AFM image shown in Figure 1S of the SI. The control of the transmission angle of light beams is based on the EOT effect on the Ag nanograting and the LC-tuned SPs. The light transmission process of EOT includes a

Received: March 24, 2014

Published: July 22, 2014

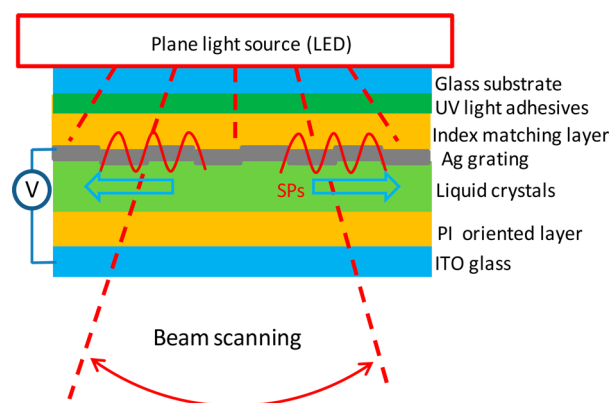


Figure 1. Schematic diagram of the beam angle modulator based on the EOT effect and the LC-tuned SPs.

coupling process (from light to SPs) and a decoupling process (from SPs to light). The LED as a plane light source illuminates the Ag nanograting. The Ag nanograting covers a large range of the incident angle of the LED. SPs are first excited at the interface between the Ag grating and the matching layer. Then, the evanescent wave of the SPs penetrates through the Ag grating and further excites the SP wave at the interface between the Ag grating and the LC layer. Subsequently, the SP wave would decouple to directional light due to the diffraction of the

Ag grating. The light transmission angle exactly equals the SPR angle, which can be tuned by changing the RI of the LC. Therefore, the angle scanning of the transmission beams could be achieved via the continuous adjustment of the applied voltages on the LC layer. It should be noted that the light transmission will be greatly enhanced if the SP waves existing on both sides of the Ag grating match well.²² Thus, the RI of the matching layer should be close to that of the LC.

Plasmonic Characteristics of the Angle Modulator.

The angles of transmission light depend on the resonant modes of SPs.^{23,24} Hence, we first studied on the plasmonic characters of this angle modulator using angle-resolved spectroscopy. Figure 2a shows that the detection geometry is a reflection mode. The angle-resolved reflection spectra, also known as the dispersion relation curves of SPs, are plotted in Figure 2b,c. It can be noted that there are only two SPR bands in the visible light range: +1 mode at short wavelength and -1 mode at long wavelength (more detailed theoretical analysis can be found in SI). The SPR bands have a quasi-linear dispersion, which is beneficial to the modulation of the SPR angles and wavelengths on this device. Comparing Figure 2b and c, one can find that the SPR bands obviously shifted to longer wavelengths when an electric field of $2.4 \text{ V}/\mu\text{m}$ was applied to the LC layer. This is caused by the increase of the RI of LC layer under an electric field. Correspondingly, the SPR angle at a fixed wavelength moved to lower degrees. For instance, along the black dashed

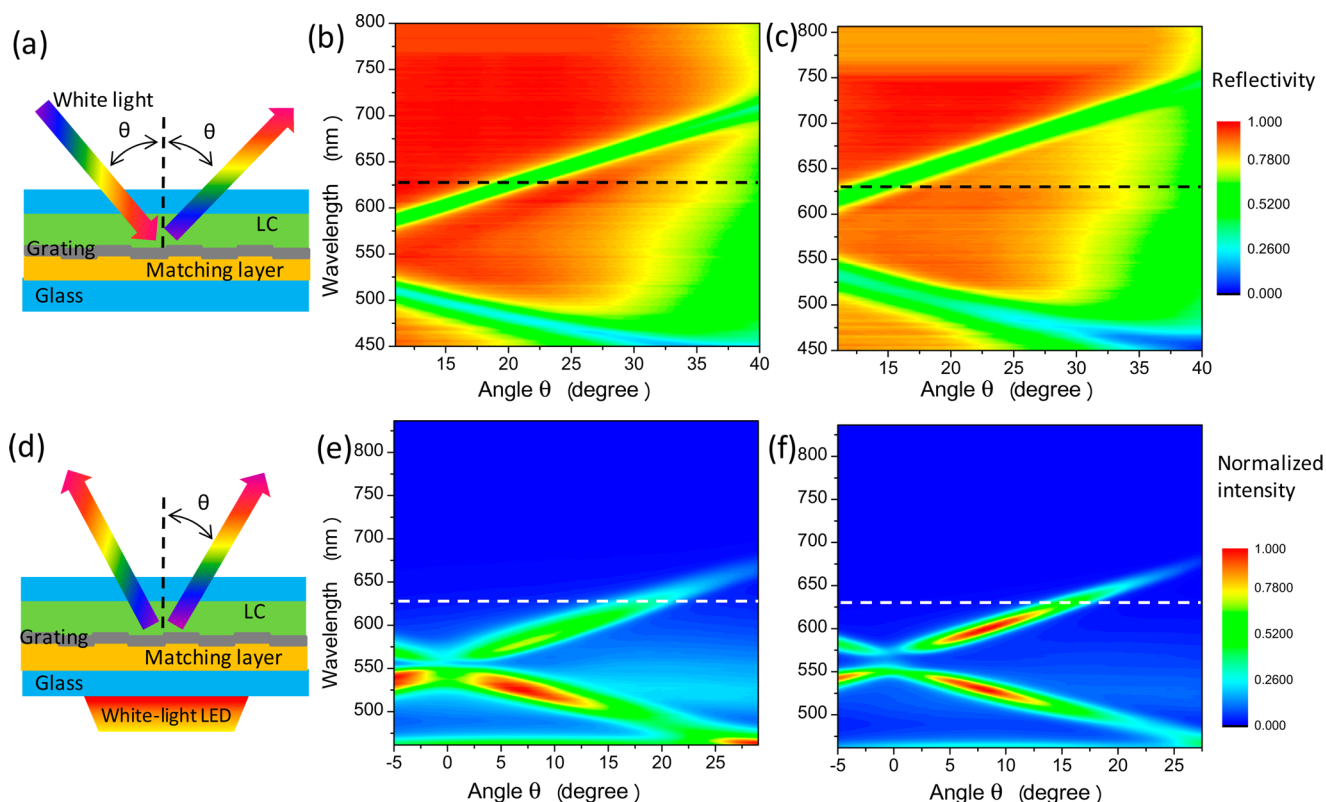


Figure 2. Plasmonic characters of the angle modulator. (a) Schematic diagram for the determination of the dispersion relations of SPs on the Ag nanograting. (b, c) Angle-resolved reflection spectra of the angle modulator when 0.0 and $2.4 \text{ V}/\mu\text{m}$ were applied on the LC layer, respectively. The colors stand for the reflectivity, which is a calibrated value to the reflection spectrum of an Ag mirror. The reflection spectra from 0 to 10° were absent due to the existence of an inner hindrance between the illumination and detection devices. (d) Schematic diagram for detecting the angle-resolved transmission spectra on the angle modulator. (e, f) Angle-resolved transmission spectra on the angle modulator when 0.0 and $2.4 \text{ V}/\mu\text{m}$ were applied on the LC layer, respectively. The colors stand for the light intensity. The transmission spectra were normalized by the maximum light intensities of the light source (an ordinary phosphor-based white-light LED). Dashed lines in (b), (c), (e), and (f) mark the wavelength of 630 nm. The profiles along the dashed lines in (e) and (f) are in the SI.

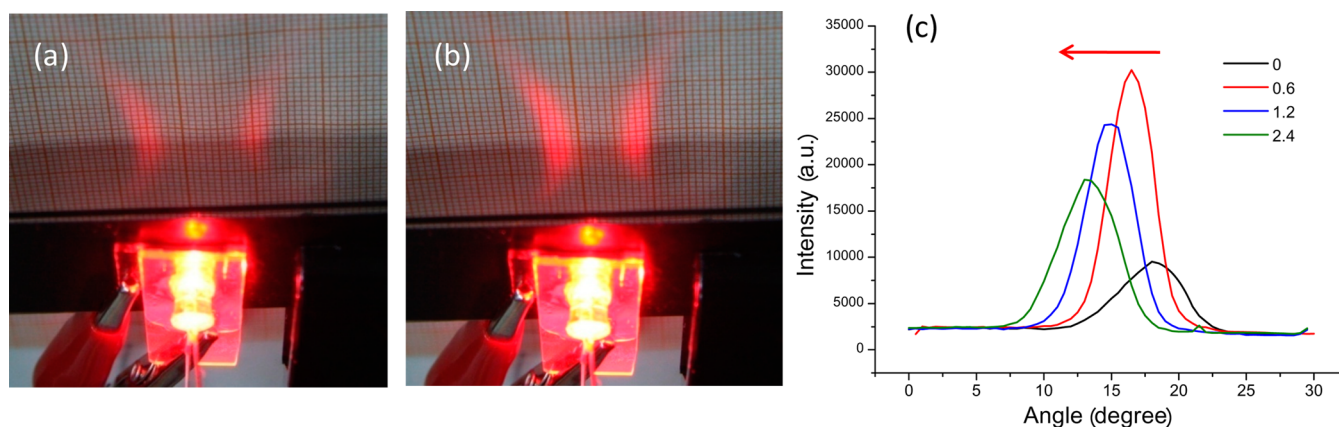


Figure 3. Angle modulation of light beams via voltage signals. (a, b) Photos of the emission patterns (the red spots on the screen) before and after applying an electric field of $2.4 \text{ V}/\mu\text{m}$ on the LC layer. The distance from the LED to the screen (coordinate paper) was approximately 3 cm and the coordinate paper has a 1 mm grid. (c) The light fields of the plasmonic device at 630 nm wavelength under different electric fields obtained by the angle-resolved spectroscopy.

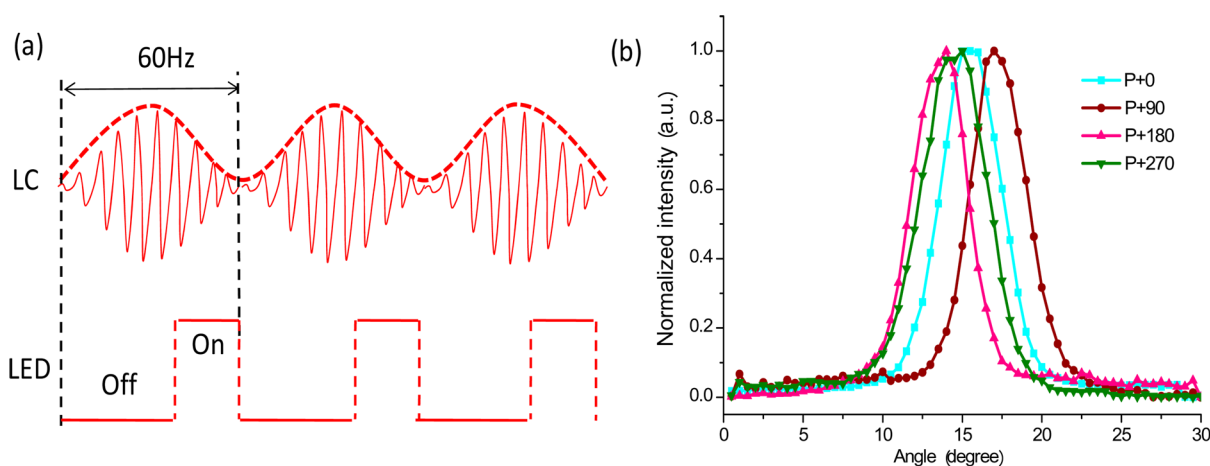


Figure 4. Dynamic angle modulation of light beams via voltage signals. (a) Schematic diagram of the driving signal for LC and LED. The driving signal for the LC is an amplitude-modulated sinusoidal wave. The frequency of the sinusoidal wave was 1000 Hz. The amplitude-modulated frequency was 60 Hz and the modulation depth was 100%. The driving signal for the on–off time of LED was a square wave (the range was set as 0–3 V and the fill factor of 3 V was 20%) at 60 Hz. (b) The dynamic modulation of light field were obtained by varying the phase difference between the driving signals over LC and LED. The legends represent the phase delay of the LED driving signals (the initial phase difference is P).

lines showing a certain wavelength at 630 nm, the SPR band shifted from about 20 to 13° before and after the electric field was applied (Figure 2b,c). The angle-resolved transmission spectra were also obtained under the detection geometry of Figure 2d. A white LED illuminates the Ag nanograting in a broad range of incident angles. Figure 2e,f shows the angle-resolved transmission spectra under different applied voltages. The transmission bands caused by EOT are obvious and they comply with the dispersion relation of SPs. Similar to the red shifts of the SPR bands in Figure 2b,c, the transmission bands shifted to longer wavelengths under an electric field of $2.4 \text{ V}/\mu\text{m}$. At the same time, the emission directions changed to smaller angles at a fixed wavelength (along the dashed lines). To clearly display the effect of angle modulation, in the following study, a monochrome LED with the emission wavelength of 630 nm and the full width at half-maximum (fwhm) of around 10 nm was used as a light source in this angle modulator.

Angle Modulation of Light Beams via Voltage Signals.

Figure 3a,b shows the photos of the transmission patterns (the red spots on the screen) through the multilayered plasmonic

device before and after applying an electric field of $2.4 \text{ V}/\mu\text{m}$ on the LC layer. The patterns are two symmetric crescents. These two conjugated beams result from the SP-induced EOT effect on the nanograting (detailed discussion is shown in SI). Comparing Figure 3a and b, one can find the crescent patterns become closer under an electric field, indicating the decrease of the transmission angles. Video 1 in the SI shows the dynamic angle modulation of the beams.

The light intensity distributions obtained by the angle-resolved spectroscopy are shown in Figure 3c. The emission angle is 18° at $0 \text{ V}/\mu\text{m}$, and the angles decrease as the electric field increases. The emission angle shifts to 13° at $2.4 \text{ V}/\mu\text{m}$, which indicates that the tunable range of the emission angles is about 5° . This angle range is smaller than the theoretical expectation that the tunable range would be around 10° when the RIs of LC change from 1.52 to 1.71 (from the ordinary light refractivity index of LC to the extraordinary light refractivity index of LC) based on the coupling conditions on a grating (see Part 5 in the SI).¹² In this ideal condition, the optical axes of the LC molecules should vary to a vertical orientation. However, in practice, the LC molecules close to the metal

surface cannot rotate to the expected orientation due to the anchorage force, causing the RI tunable range of LC smaller than the theoretical prediction. Therefore, the tunable angle range of transmission beams is less than 10° experimentally.

Light Beam Scanning at a High Refresh Rate. The LC-tuned plasmonic device could modulate light in a high refresh rate. Figure 4a shows the schematic diagram of the driving signals on LC and LED. The driving signal on LC was an amplitude-modulated sinusoidal wave with a frequency of 60 Hz and a modulation depth of 100%. Under this driving signal, the transmission angles of light beams can be scanned in a range of 5 degrees at a refresh rate of 60 Hz. The directions of light beams could be tuned by controlling the on–off time of the LED, which is the phase difference. The driving signal to control the on–off time of the LED is a square wave (0 and 3 V, the fill factor of 20% at 3 V) with a rate of 60 Hz. Since two signals of driving LC and LED are from two independent channels of a function wave generator, there is an initial phase difference (P) between two signals (Figure 4b). We adjusted the phase of the LC driving signal and delayed the phase of the LED driving signal to offset the phase difference. As expected, the light beams emitted at one direction when the LED turned on once in one scanning cycle of the LC and the emission directions varied with the phase difference.

Angle Modulation of Beams Illuminated by a Focused Light Beam to Attain Unidirectional Beams. The unidirectional beams have more practical applications than the crescent-shaped beams. We aim to obtain the unidirectional beams by using a focused light beam instead of a plane light source. As shown in Figure 5a, the incident angles cover from 0 to $+25^\circ$, which is different from the case in Figure 1a where the incident angles cover almost from -90 to $+90^\circ$. Thus, the transmission beams only exist in this range and the conjugate

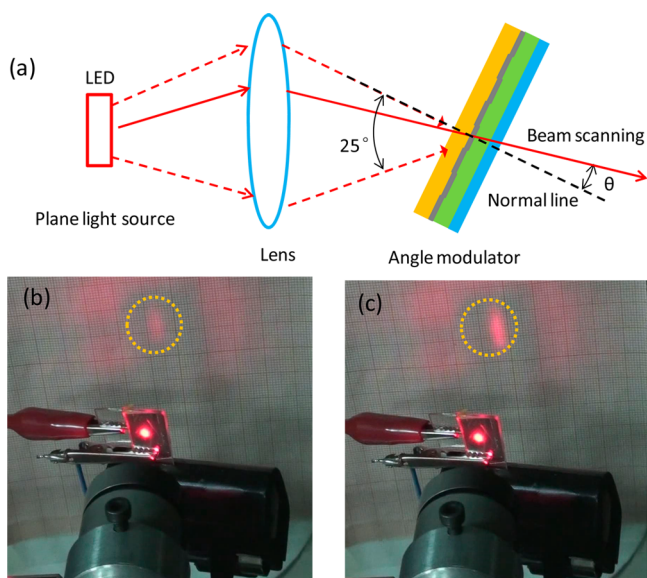


Figure 5. Angle modulation of light beams illuminated by a focused light beam. (a) Geometry configuration of the angle modulation of beams illuminated by a focused light beam. (b, c) The photos show the shift of the emission beams before and after applying an electric field of $2.4 \text{ V}/\mu\text{m}$ on the LC layer. The yellow dashed circles highlight the light spots of the transmission beams. The red areas out of the yellow circles are stray light from the light source. A video showing the angle modulation of light beams in this configuration is provided in the SI.

beams disappear. As shown in Figure 5b, there is only one light spot on the screen, differing from the two symmetric crescent patterns in Figure 3. Furthermore, the beam angle can be tuned by applying a repetitive voltage signal in the same mode as that used in Figure 3 (see the video in SI).

Possible Application for a 3D Image. 3D display is an attractive visualization technology that provides an efficient tool to understand complex high-dimensional data and objects, for example, scientific computing, computer-aided design, and medical imaging.^{25–27} To form an autostereoscopic 3D display, the emission angles of light beams from a 3D pixel should be modulated.^{25–27} This plasmonic angle modulator which can achieve light beam scanning presents a possibility to construct a high-resolution 3D display.

The angle modulation of light is the key technology to generate a realistic image. Traditional display devices only show 2D images that lack depth (i.e., the third dimension) information since the pixels only express the position and brightness of an image. To form an autostereoscopic 3D display, the emission angle of rays from a 3D pixel should be modulated. The basic technology of 3D displays modulates light in two different directions via a parallax barrier screen, which presents offset images that project separately to the left and right eyes. However, the motion parallax cannot be generated via this technology.²⁸ To obtain more realistic 3D images, each 3D display pixel should emit a number of directionally light beams, generating different images in multiple (different) angular positions. This is the concept of the multiview autostereoscopic 3D display technology. In the present multiview 3D technology, a single 3D pixel which integrates multiple directional emitters are usually used.^{22,29} However, numerous directional emitters (as the subpixels) contained in one pixel are not beneficial for decreasing the size of a pixel. For instance, in order to construct a display with N views, the resolution of an individual view is essentially $1/N$ of the original display resolution which limits the resolution of the images. To solve this, the plasmonic angle modulator may open a new opportunity to obtain the directionally varying light in micro/nanoscale. As shown in Figure 6, an array involving

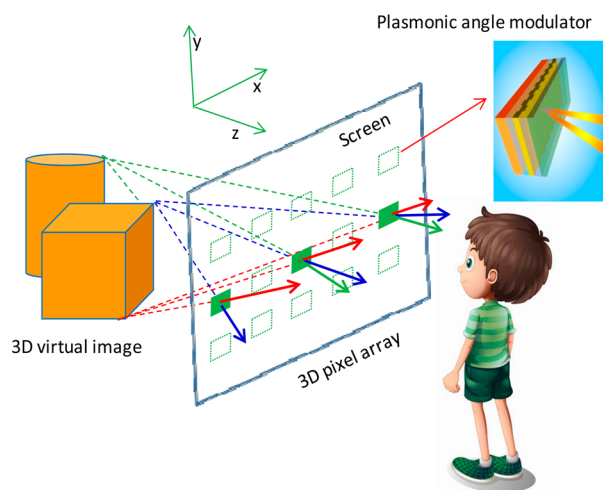


Figure 6. Schematic diagram for the multiview 3D display achieved by reproducing the light fields (the light intensities at different angles) of objects via the plasmonic angle modulator array. The beams with different colors represent the scattering beams from different locations of the virtual objects.

plasmonic angle modulators was designed and the light beam directions could be controlled by the LC-tuned SPs. The scattering light field of an object could be reproduced by this plasmonic elements array. The utilization of the designed plasmonic angle modulators is advantageous to decrease the size of 3D pixels and improve the resolution of 3D images above the traditional 3D pixels.

In addition, the angle modulation range was considered. For our designed angle modulator, the tunable range was 5° at a 60 Hz refresh rate, which allows for the requirement of a particle pixel element for a 3D display. The angle modulation range is decided by the viewing field (i.e., the viewing angle). If we watch the 3D TV at a distance of around 2 m, the inclined angle of two light beams should be more than 3° to guarantee the projected views different for two eyes (the distance between two human eyes is about 0.1 m). Thus, a 5° modulation range is wide enough to generate 3D images at a viewing distance of around 2 m. However, the further improvement of the tunable range is very necessary because a wider viewing angle allows many people watching 3D images at the same time. Moreover, a refresh rate of 60 Hz was achieved, which guarantees that naked eyes cannot perceive the flickering of images, achieving a quasi-static 3D image for eyes.

One more promising thing is that this technique has the possibility to achieve the colored 3D display. More statements are shown in the SI.

Other Applications. The beam angle modulation based on the LC-tuned SPs is also in great demand in nano-optic fields. Although beam steering can be achieved by phase-array optics (e.g., using spatial light modulator) and microelectromechanical systems using micromirrors, the difficulty in the fabrication and the diffraction limit restricts their applications in subwavelength scale. With the development of integrated optics technique, the plasmon-based angle modulators in a nanosize will show their attractive prospects in photocommunication and optical detection fields.

CONCLUSION

An active angle modulation device of light beams based on the LC-tuned SPs is proposed, which has great application potentials in the multiview 3D display. The plasmonic angle modulator has a multilayered structure, containing an Ag nanograting film to couple SPs and a LC cell attaching to Ag grating to tune SPs by means of voltage signals. The videos and angle-resolved spectra show that this angle modulator can efficiently regulate the light beam angles in a 5° range at a refresh rate of 60 Hz. This prototypical device opens a new opportunity to achieve multiview 3D display. It may miniaturize the pixel size and improve the resolution of 3D display. In addition, this plasmonic angle modulator also has wide applications in other fields, such as photocommunication, optical detection, beam steering, and so on.

METHODS

Preparing the Plasmonic Angle Modulator. (1) Fabrication of the Ag nanograting film and the matching layer. The Ag film with grating pattern was prepared by vacuum evaporation depositing a 100 nm thickness Ag film (at a speed of 0.2 nm/s) on a Bluray disc (RiTEK Company). Then, a polyimide (PI) solution (2 wt % PI in pyrrolidone) as a matching layer was spin-coated on one side of the Ag grating (3000 rad/min, about 100 nm in thickness). The Ag grating

with the PI film was heated to 80°C for 30 min to obtain a thermosetting coating. The RI of the fixed PI film is 1.7. Finally, the Ag layer with PI film was fixed and supported on a glass slide using ultraviolet curing adhesive and then peeled off from the Bluray disc.

(2) Construction of the LC cell. The LC cell is composed of a film spacer (50 μm in thickness) and an ITO glass with the PI oriented film and the Ag grating film. We first spin-coated the PI solution (2 wt %) on an ITO glass slide at 3000 rad/min and then heated them at 200°C for 60 min. To obtain oriented grooves for LC, the PI oriented film needs to be repeatedly rubbed along the direction of the grooves of the metal grating with a nonwoven fabric for at least 20 times. The LC cell was constructed with the treated ITO glass, PI film spacer and the Ag nanograting film with the matching layer. After that, the LC (TEB50, from ChengzhiYonghua Display Materials Co., Ltd.) was filled into the LC cell at a temperature of 65°C by capillary force.

Angle Modulation of Light Beams Illuminated by a Plane Light Source (LED). A LED with a flat-end (emission peak at 630 nm, fwhm of 10 nm) was attached to the glass substrate side using ultraviolet curing adhesive as the plane light source. The electric signal to drive the LC cell is an amplitude-modulated sinusoidal wave from a function waveform generator (dual channels, RIGOL Technologies, Inc.) with a transformer to improve the voltage. The electric signal to drive the LED is a square wave from the second channel of the function waveform generator.

The angle-resolved spectrum detection system for measuring the reflection light and transmission light has been reported in our previous work.³⁰ A detection lens with the numerical aperture of 0.02 was used to achieve high angular resolution.

ASSOCIATED CONTENT

Supporting Information

(1) The morphology of the Ag nanograting; (2) Angle modulation of beams illuminated by a plane light source (Video 1); (3) Angle modulation of beams illuminated by a focused beam (Video 2); (4) Colored 3D display based on the plasmonic angle modulator; (5) The SP modes on a grating; (6) Mechanism of the LC-tuned SPs; (7) Transmission spectra of the angle modulator at 630 nm when applying different voltages; (8) Explanation on the emergence of a crescent shaped light pattern; and (9) Discussion on the dependence of the geometric parameters of the grating for the angle modulation. This material is available free of charge via the Internet at <http://pubs.acs.org>.

AUTHOR INFORMATION

Corresponding Author

*Tel.: +86-431-85168505. Fax: +86-431-85193421. E-mail: xuwq@jlu.edu.cn.

Notes

The authors declare no competing financial interest.

ACKNOWLEDGMENTS

This work was supported by the National Instrumentation Program (NIP) of the Ministry of Science and Technology of China (Grant No. 2011YQ03012408), and National Natural Science Foundation of China (NSFC; Grant Nos. 21373096, 21073073, and 91027010).

■ REFERENCES

- (1) Barnes, W. L.; Dereux, A.; Ebbesen, T. W. Surface Plasmon Subwavelength Optics. *Nature* **2003**, *424*, 824–830.
- (2) Kosako, T.; Kadoya, Y.; Hofmann, H. F. Directional Control of Light by a Nano-Optical Yagi-Uda Antenna. *Nat. Photonics* **2010**, *4*, 312–315.
- (3) Baron, A.; Devaux, E.; Rodier, J. C.; Hugonin, J. P.; Rousseau, E.; Genet, C.; Ebbesen, T. W.; Lalanne, P. Compact Antenna for Efficient and Unidirectional Launching and Decoupling of Surface Plasmons. *Nano Lett.* **2011**, *11*, 4207–4212.
- (4) Devilez, A.; Stout, B.; Bonod, N. Compact Metallo-Dielectric Optical Antenna for Ultra Directional and Enhanced Radiative Emission. *ACS Nano* **2010**, *4*, 3390–3396.
- (5) Jun, Y. C.; Huang, K. C. Y.; Brongersma, M. L. Plasmonic Beaming and Active Control over Fluorescent Emission. *Nat. Commun.* **2011**, *2*, 283.
- (6) Huang, K. C. Y.; Seo, M. K.; Huo, Y. J.; Sarmiento, T.; Harris, J. S.; Brongersma, M. L. Antenna Electrodes for Controlling Electroluminescence. *Nat. Commun.* **2012**, *3*, 1005.
- (7) Lezec, H. J.; Degiron, A.; Devaux, E.; Linke, R. A.; Martin-Moreno, L.; Garcia-Vidal, F. J.; Ebbesen, T. W. Beaming Light from a Subwavelength Aperture. *Science* **2002**, *297*, 820–822.
- (8) Aouani, H.; Mahboub, O.; Bonod, N.; Devaux, E.; Popov, E.; Rigneault, H.; Ebbesen, T. W.; Wenger, J. Bright Unidirectional Fluorescence Emission of Molecules in a Nanoaperture with Plasmonic Corrugations. *Nano Lett.* **2011**, *11*, 637–644.
- (9) Raether, H. *Surface Plasmons on Smooth and Rough Surfaces and on Gratings*; Springer-Verlag: Hamburger, Germany, 1986; Ch. 2.
- (10) Kossyrev, P. A.; Yin, A. J.; Cloutier, S. G.; Cardimona, D. A.; Huang, D. H.; Alsing, P. M.; Xu, J. M. Electric Field Tuning of Plasmonic Response of Nanodot Array in Liquid Crystal Matrix. *Nano Lett.* **2005**, *5*, 1978–1981.
- (11) Liu, Y. J.; Leong, Eunice S. P.; Wang, B.; Teng, J. H. Optical Transmission Enhancement and Tuning by Overlying Liquid Crystals on a Gold Film with Patterned Nanoholes. *Plasmonics* **2011**, *6*, 659–664.
- (12) Li, H. B.; Xu, S. P.; Gu, Y. J.; Wang, K.; Xu, W. Q. Active Modulation of Wavelength and Radiation Direction of Fluorescence via Liquid Crystal-Tuned Surface Plasmons. *Appl. Phys. Lett.* **2013**, *102*, 051107.
- (13) Xie, J.; Zhang, X. M.; Peng, Z. H.; Wang, Z. H.; Wang, T. Q.; Zhu, S. J.; Wang, Z. Y.; Zhang, L.; Zhang, J. H.; Yang, B. Low Electric Field Intensity and Thermotropic Tuning Surface Plasmon Band Shift of Gold Island Film by Liquid Crystals. *J. Phys. Chem. C* **2012**, *116*, 2720–2727.
- (14) Li, J.; Ma, Y.; Gu, Y.; Khoo, I. C.; Gong, Q. H. Large Spectral Tunability of Narrow Geometric Resonances of Periodic Arrays of Metallic Nanoparticles in a Nematic Liquid Crystal. *Appl. Phys. Lett.* **2011**, *98*, 213101.
- (15) Khatua, S.; Chang, W. S.; Swanglap, P.; Olson, J.; Link, S. Active Modulation of Nanorod Plasmons. *Nano Lett.* **2011**, *11*, 3797–3802.
- (16) Li, H. B.; Xu, S. P.; Gu, Y. J.; Wang, H. L.; Ma, R. P.; Lombardi, J. R.; Xu, W. Q. Active Plasmonic Nanoantennas for Controlling Fluorescence Beams. *J. Phys. Chem. C* **2013**, *117*, 19154–19159.
- (17) Ebbesen, T. W.; Lezec, H. J.; Ghaemi, H. F.; Thio, T.; Wolff, P. A. Extraordinary Optical Transmission through Sub-Wavelength Hole Arrays. *Nature* **1998**, *391*, 667–669.
- (18) Garcia-Vidal, F. J.; Martin-Moreno, L.; Ebbesen, T. W.; Kuipers, L. Light Passing through Subwavelength Apertures. *Rev. Mod. Phys.* **2010**, *82*, 729–787.
- (19) Xu, T.; Wu, Y.; Luo, X.; Guo, L. J. Plasmonic Nanoresonators for High-Resolution Colour Filtering and Spectral Imaging. *Nat. Commun.* **2010**, *1*, 59.
- (20) Barnes, W. L.; Murray, W. A.; Dintinger, J.; Devaux, E.; Ebbesen, T. W. Surface Plasmon Polaritons and Their Role in the Enhanced Transmission of Light Through Periodic Arrays of Subwavelength Holes in a Metal Film. *Phys. Rev. Lett.* **2004**, *92*, 107401.
- (21) Genet, C.; Ebbesen, T. W. Light in Tiny Holes. *Nature* **2007**, *445*, 39–46.
- (22) Krishnan, A.; Thio, T.; Kim, T. J.; Lezec, H. J.; Ebbesen, T. W.; Wolff, P. A.; Pendry, J.; Martin-Moreno, L.; Garcia-Vidal, F. J. Evanescently Coupled Resonance in Surface Plasmon Enhanced Transmission. *Opt. Commun.* **2001**, *200*, 1–7.
- (23) Pang, Y.; Genet, C.; Ebbesen, T. W. Optical Transmission through Subwavelength Slit Apertures in Metallic Films. *Opt. Commun.* **2007**, *280*, 10–15.
- (24) Lee, J. W.; Seo, M. A.; Sohn, J. Y.; Ahn, Y. H.; Kim, D. S.; Jeoung, S. C.; Lienau, C.; Park, Q. H. Invisible Plasmonic Meta-Materials through Impedance Matching to Vacuum. *Opt. Express* **2005**, *13*, 10681–10687.
- (25) Geng, J. Three-Dimensional Display Technologies. *Adv. Opt. Photonics* **2013**, *5*, 456–535.
- (26) Takaki, Y. High-Density Directional Display for Generating Natural Three-Dimensional Images. *Proc. IEEE* **2006**, *94*, 654–663.
- (27) Urey, H.; Chellappan, K. V.; Erden, E.; Surman, P. State of the Art in Stereoscopic and Autostereoscopic Displays. *Proc. IEEE* **2011**, *99*, 540–555.
- (28) Geng, J. Structured-Light 3D Surface Imaging: a Tutorial. *Adv. Opt. Photonics* **2011**, *3*, 128–160.
- (29) Kwon, H.; Choi, H. J. A Time-Sequential Multi-View Autostereoscopic Display without Resolution Loss Using a Multi-Directional Backlight Unit and an LCD Panel. *Proc. SPIE* **2012**, *8288*, 82881Y.
- (30) Li, H. B.; Xu, S. P.; Liu, Y.; Gu, Y. J.; Xu, W. Q. Directional Emission of Surface-Enhanced Raman Scattering Based on a Planar-Film Plasmonic Antenna. *Thin Solid Films* **2012**, *520*, 6001–6006.